Glaucoma

Recent Structural Alteration of the Peripheral Lamina Cribrosa Near the Location of Disc Hemorrhage in Glaucoma

Eun Ji Lee,[1] Tae-Woo Kim,[1] Mijin Kim,[1] Michaël J. A. Girard,[2,3] Jean Martial Mari,[4] and Robert N. Weinreb[5]

[1]Department of Ophthalmology, Seoul National University College of Medicine, Seoul National University Bundang Hospital, Seongnam, Korea
[2]Department of Bioengineering, National University of Singapore, Singapore
[3]Singapore Eye Research Institute, Singapore
[4]INSERM U1032, Université de Lyon, Lyon, France
[5]Hamilton Glaucoma Center and Shiley Eye Center, Department of Ophthalmology, University of California San Diego, La Jolla, California, United States

PURPOSE. We investigated whether disc hemorrhage (DH) is associated with the recent structural alteration of the peripheral lamina cribrosa (LC) as assessed by enhanced depth imaging (EDI) spectral-domain optical coherence tomography (SD-OCT).

METHODS. Serial horizontal B-scan images were obtained by EDI SD-OCT from primary open-angle glaucoma (POAG) patients before and after the detection of DH (DH group, $n = 45$), and those who had no DH during the 1-year scan interval (non-DH group, $n = 36$). The images were processed using compensation and contrast enhancement. Then, 11 radial OCT images centered on the optic disc were generated from the 3-dimensionally reconstructed volume image. A recent structural alteration of the LC was defined when either the outward deformation of the anterior LC surface or radial disruption of the LC was identified in the temporal periphery.

RESULTS. A recent structural alteration of the LC was found in 40 (88.9%) eyes in the DH group versus 4 (11.1%) eyes in the non-DH group. The amount of maximum outward deformation (55.82 ± 34.60 vs. 20.15 ± 4.28 μm) and radial disruption (69.87 ± 46.74 vs. 18.31 ± 1.17 μm) was larger in the DH group than in the non-DH group. The maximum LC alteration was observed within 1 clock-hour distance from the location of DH in all 40 eyes.

CONCLUSIONS. The peripheral LC exhibited a recent alteration in eyes with DH. The alteration was correlated spatially with the location of the DH. These findings suggest that DH may result from microvascular damage incurred from alteration of the LC near its insertion.

Keywords: lamina cribrosa, disc hemorrhage, spectral-domain optical coherence tomography, primary open-angle glaucoma

D isc hemorrhage (DH) is an important risk factor for development[1,2] and progression of glaucoma.[3-9] It often precedes nerve fiber layer damage,[7,10-12] optic disc changes,[5] or visual field defects.[6,7,12,13] The DH is detected in approximately 2% to 28% of glaucomatous eyes,[14-19] while rarely found in normal eyes.[14,15] Furthermore, location of DH is highly correlated with the location of the RNFL defect[11] or neural rim notches,[20] and predicts the location of RNFL defect, which develops later in eyes that had DH.[21]

The pathogenesis of DH remains to be elucidated. Quigley et al.[22] suggested that DH results from microvascular disruption, which occurs in the process of backward bowing of the lamina cribrosa (LC). This idea is in line with earlier reports by Emery et al.[23] and Radius et al.,[24] which suggested that a predictable pattern of connective tissue (LC) deformation underlies the glaucomatous cupping. Nitta et al.[25] proposed that the degenerative changes of retinal nerve fiber layer and damage to the capillary network surrounding the border of retinal

nerve fiber layer defect could produce DH. These hypotheses indicate that DH results from the mechanical disruption of the capillaries secondary to stretching or degenerative change. Recently, Yang et al.[26] demonstrated the posterior migration of the LC insertion in early experimental glaucomatous monkey eyes, an observation in support of DH being derived from the microvascular disruption. In addition, other investigators suggested that the DH is derived from the hemodynamic disturbance including microinfarction in the optic disc, disorder of retinal circulation, or decrease in capillary perfusion.[27-30] Increased levels of circulating endothelin-1[31] and matrix metalloproteinase-9,[32] which may disturb the blood–retinal barrier, also have been suggested to be involved in the development of DH.

With the emergence of spectral domain optical coherence tomography (SD-OCT) especially with enhanced depth imaging (EDI) technique, it became possible to image the LC in patients. Using EDI-OCT, several studies have demonstrated localized

structural alteration of the peripheral LC, including focal LC defect and pit.[33–36] The focal LC defects were spatially correlated with localized neuroretinal rim loss,[33,34] visual field defects,[33] and retinal nerve fiber layer defects.[35] An association of DH with focal LC defects also has been reported.[36] Although these studies were performed in a cross-sectional design, they demonstrate that the glaucomatous optic neuropathy involves not only the loss of retinal nerve fibers and prelaminar tissue, but also the damage of the underlying LC, as demonstrated in the histologic studies.[26,37]

The purpose of the present study was to investigate whether the recent structural alteration of the peripheral LC is associated with DH. To do this, EDI-OCT images obtained before and after the DH were compared. The recent alteration of the LC was identified when the deformation, disruption, and defect (partial thickness disruption) of the LC was found on the post-DH image compared to the pre-DH image. To our knowledge, comparison of the LC configuration before and after the DH never has been performed.

METHODS

This investigation was based on the Lamina Cribrosa Exploration Study (LCES) and Investigating Glaucoma Progression Study (IGPS), ongoing prospective studies in the Seoul National University Bundang Hospital Glaucoma Clinic.

The study was approved by Seoul National University Bundang Hospital Institutional Review Board and conformed to the Declaration of Helsinki. Informed consent was obtained from all patients.

Study Subjects

Patients who were enrolled in the LCES and IGPS underwent a complete ophthalmic examination, including visual acuity assessment, refraction, slit-lamp biomicroscopy, gonioscopy, Goldmann applanation tonometry, and dilated stereoscopic examination of the optic disc. They also underwent central corneal thickness measurement (Orbscan II; Bausch & Lomb Surgical, Rochester, NY, USA), axial length measurement (IOL Master ver. 5; Carl-Zeiss Meditec, Dublin, CA, USA), stereo disc photography, SD-OCT (Spectralis OCT; Heidelberg Engineering GmbH, Heidelberg, Germany), and standard automated perimetry (Humphrey Field Analyzer II 750; 24-2 Swedish interactive threshold algorithm; Carl-Zeiss Meditec).

To be included in either study, subjects were required to have a best corrected visual acuity of ≥20/40, spherical refraction of −8.0 to +3.0 diopters, and cylinder correction of ≤±3.0 diopters. Those with a history of ocular surgery other than cataract extraction and glaucoma surgery, and intraocular disease (e.g., diabetic retinopathy or retinal vein occlusion) or neurologic disease (e.g., pituitary tumor) that could cause visual field loss were excluded. Eyes that received cataract surgery or glaucoma surgery between the scan interval also were excluded.

All patients included in the LCES and IGPS were followed up every 3 to 6 months with regular follow-up fundus photography, SD-OCT retinal nerve fiber layer thickness measurement, and visual field testing being performed at 6-month to 1-year intervals. Optic disc scan using EDI SD-OCT was performed at 1- to 2-year intervals.

To be included in the present study as a DH group, patients were required to have POAG, and to have at least one DH observed with photography between serial EDI SD-OCT optic disc scans. The condition of POAG was defined as the presence of glaucomatous optic nerve damage and associated visual field defect without ocular disease or conditions that may elevate the IOP. A DH was defined as an isolated hemorrhage seen on the disc tissue or in the peripapillary retina connected to the disc rim.[5] Glaucomatous visual field defect was defined as outside normal limits on the glaucoma hemifield test; or three abnormal points with $P < 5\%$ being normal, one with $P < 1\%$ by pattern deviation; or pattern SD of $P < 5\%$ if the visual field otherwise was normal, confirmed on two consecutive tests. Eyes with a history of DH previously observed before the baseline EDI SD-OCT optic disc scan were excluded.

Patients for the non-DH group were recruited among POAG patients who had 2 optic disc scans within 1 year. To be included, they were required to have had regular follow-up with less than 4 months intervisit interval, and no observable DH during the scan interval. This group was matched with DH group for age, visual field mean deviation (MD), IOP at baseline and follow-up scans, and IOP fluctuation (standard deviation of IOPs obtained during the scan interval). Optic discs were examined routinely ophthalmoscopically using noncontact fundus examination lens (SuperField lens; Volk Optical, Inc., Mentor, OH, USA), and a DH recorded when observed.

EDI-OCT of the Optic Disc

The optic nerve was imaged using the EDI technique. The detail and advantage of this technology to evaluate the LC have been described previously.[33,38,39] Approximately 65 horizontal B-scan section images covering the optic disc, 30 to 34 μm apart (the scan-line distance being determined automatically by the instrument), were obtained from each eye. Each section had 42 OCT frames averaged, which provided the best trade-off between image quality and patient cooperation.[39]

Using Spectralis OCT, the images were obtainable only when the quality score was higher than 15. When the quality score did not reach 15, the image acquisition process automatically stopped and image of the respective section remained missing. Only eyes where acceptable scans (i.e., quality score > 15) obtained at more than 60 sections, and that allowed clear delineation of anterior border of the LC were included.

Compensation and Contrast Enhancement

To better visualize the peripheral LC by improving the quality of EDI images, two algorithms were applied, one to compensate for light attenuation and the other to enhance tissue contrast in EDI SD-OCT images. The detailed technique has been described and tested previously.[40,41] These algorithms significantly improved the visibility of deeper ONH tissues, including the peripapillary sclera and the LC; were able to remove blood vessel shadows; and allowed a better differentiation of tissue boundaries (especially the anterior LC boundary).[40]

3-D Construction of the Optic Disc Images and Generation of Radial Images

After processing the EDI images using compensation and contrast enhancement, the OCT data volume was constructed 3-dimensionally using image processing software (Amira 5.2.2; Visage Imaging, Berlin, Germany).[42] Then, 11 radial OCT images centered on the optic disc were generated to examine the temporal periphery of the LC (Fig. 1). Each image was radially equidistant and separated by 15°. For follow-up images, the locations were selected to correspond to those that had been selected for the baseline measurements. En face images as well as the low reflective shadow within the LC shown in B-scan images were used to confirm the correspondence of the selected images between the initial and follow-up images.[43,44]
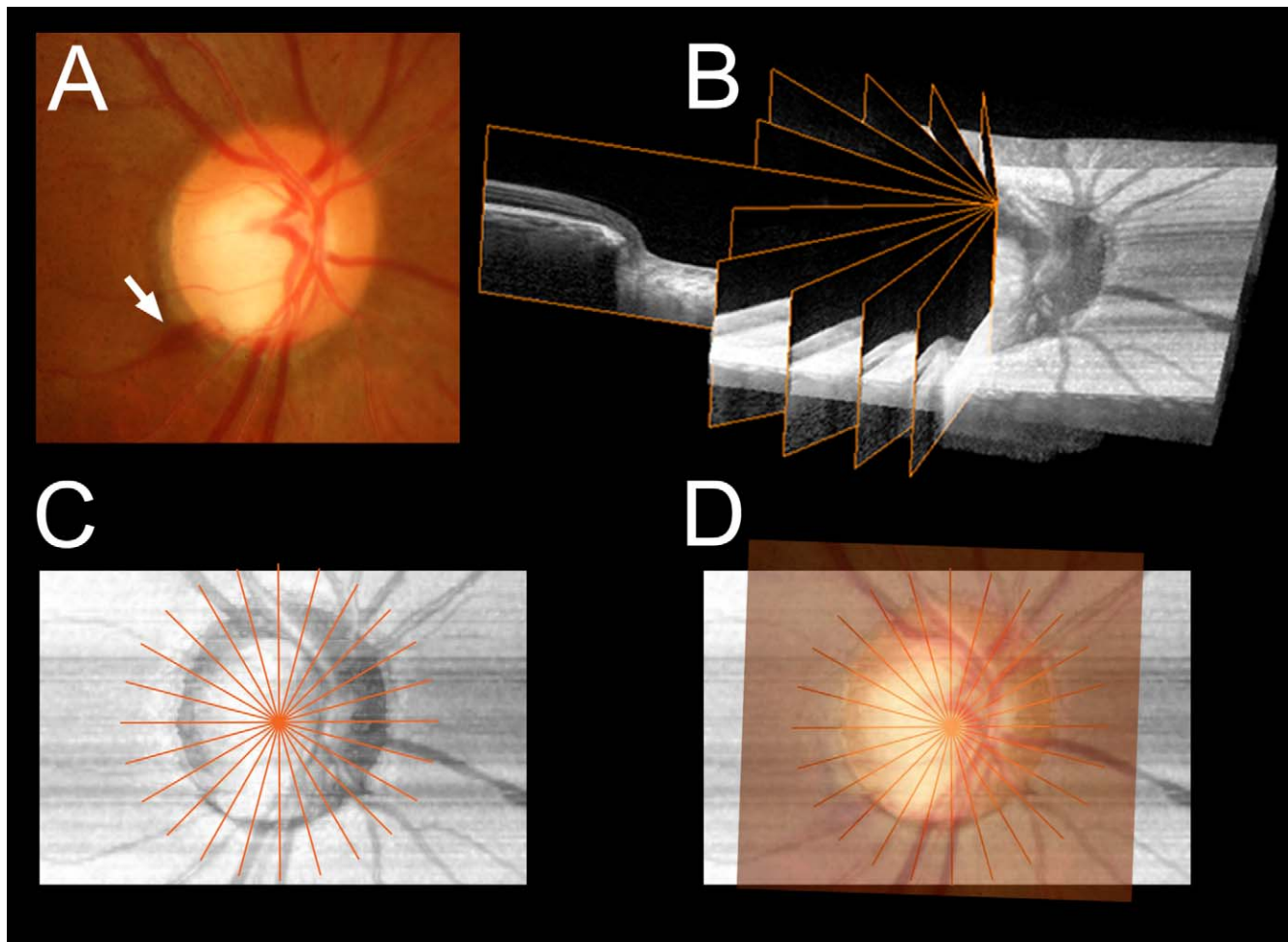
FIGURE 1. Determination of the meridian of DH. (**A**) Disc photograph of an eye having DH in the inferotemporal quadrant (*arrow*). (**B**) Maximum intensity projection image of the SD-OCT data set of the same eye with radial scan images generated as being 15° apart. Radial scans are not shown in the inferonasal quadrant to help understand the image. (**C**) En face view of the 3D image shown in (**B**). Note that the location of the radial scans are seen as the indicator of clock-hour meridians. (**D**) Combined image where fundus photograph is superimposed on the image shown in (**C**). In this case, the location of DH was determined as 7.5 o'clock.

The direction of radial images was aligned based on the right eye orientation. The superior clock-hour was 12 o'clock and the others were assigned accordingly in a clockwise manner in the right eye and counterclockwise in the left.

Determination of the Location of Disc Hemorrhage

The DH was identified on the fundus photograph. It would be ideal to use the fovea-Bruch's membrane opening (BMO) center axis (FoBMO axis) for determining the location of DH, because it allows anatomically consistent regionalization among patients.[45] However, the FoBMO axis is not visible in the EDI optic disc scanning. To overcome this limitation, the clock-hour meridian of the DH was determined using the meridian of the radial B-scan images of the SD-OCT data set after adjusting the misalignment between the fundus photograph and the SD-OCT image due to different head position or cyclotorsion during image acquisition. To do this, the disc photograph was superimposed on the en face image of the SD-OCT data set. The two images were aligned using the blood vessels as the reference on a commercial software (Photoshop CC; Adobe Systems, Inc., Mountain View, CA, USA). The clock-hour meridian of DH was determined in the superimposed meridian for the radial images (Fig. 1).

Defining the Recent Structural Alteration of the LC

The recent structural alteration of the LC was identified by comparing the baseline and follow-up OCT images. During the study, we found that the LC alteration occurred either vertically (outward deformation of the LC surface) or radially (radial disruption of the LC) at the temporal periphery near the neural canal opening.

For this study, an outward deformation was defined when the difference in the depth of the visible end of anterior LC surface between the baseline ($\alpha 1$) and follow-up images ($\alpha 2$) exceeded the test–retest variability (see Data Analysis). The depth of the visible end of anterior LC surface was measured using the Bruch's membrane level as a reference plane at each image (Figs. 2A, 3A). For eyes showing outward deformation, central LC depth additionally was measured to identify whether the outward deformation of the peripheral LC was an epiphenomenon of backward bowing of the LC. The central LC depth was determined as the distance from the reference plane to the maximally depressed point within the central half on the anterior LC surface.

A radial disruption was defined when a new cleft or the enlargement of the existing cleft exceeded the intrasample (repeated measure) variability (see Data Analysis; Figs. 2B, 3B). A recent LC alteration was defined when either the outward
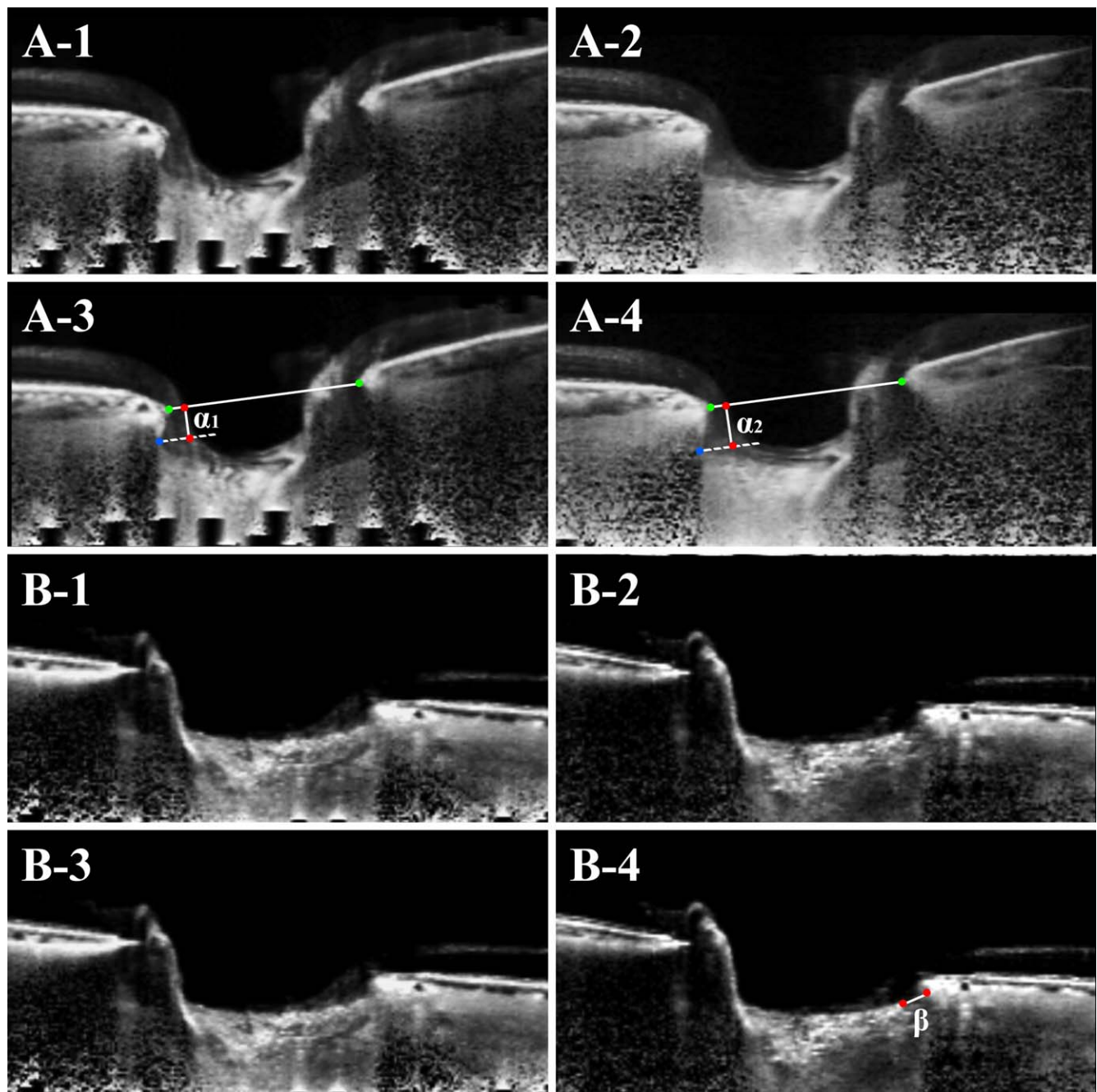
FIGURE 2. Measurement of the depth of the visible end of the anterior LC surface (**A**) and the width of LC cleft (**B**) in the temporal periphery beneath the scleral opening. *Left* and *right* images are the baseline and follow-up B-scans in each row. (**A-3**, **A-4**, **B-3**, **B-4**) Same images as (**A-1**, **A-2**, **B-1**, **B-2**) with labels, respectively. (**A-3**, **A-4**) To quantify the depth of the visible end of anterior LC surface, a *line* connecting the two BMO points (*green glyphs*) was set as the reference plane (*white solid lines*). Then, a *horizontal line* parallel to the reference plane was drawn (*white dashed lines*) from the visible end of the anterior LC surface (*blue glyphs*). This was simply to measure the perpendicular distance from the reference plane to the visible end of the anterior LC surface. The distance between the 2 *lines* was measured and compared between the baseline ($\alpha 1$) and follow-up images ($\alpha 2$). (**B-3**, **B-4**). The width of the LC cleft was measured following the curvature of LC (β).

deformation or radial disruption, or both were identified in the temporal LC. In eyes with recent LC alteration, the amount of LC alteration at the meridian where the greatest LC alteration was observed was defined as the maximum LC alteration. All measurements were performed by a single observer (EJL) who was masked to patients' clinical information, including the history of DH and the order of OCT images.

Because the LC border often was poorly recognizable in the nasal periphery (being obscured by thick neuroretinal rim or central retinal vessels), only temporal LC was considered in each radial OCT image. The 6 and 12 o'clock meridians also were excluded from the analysis because of the poor visualization of the peripheral LC at these meridians.

Data Analysis

To calculate the test–retest variability for the depth of the visible end of anterior LC surface measurement, the interses-
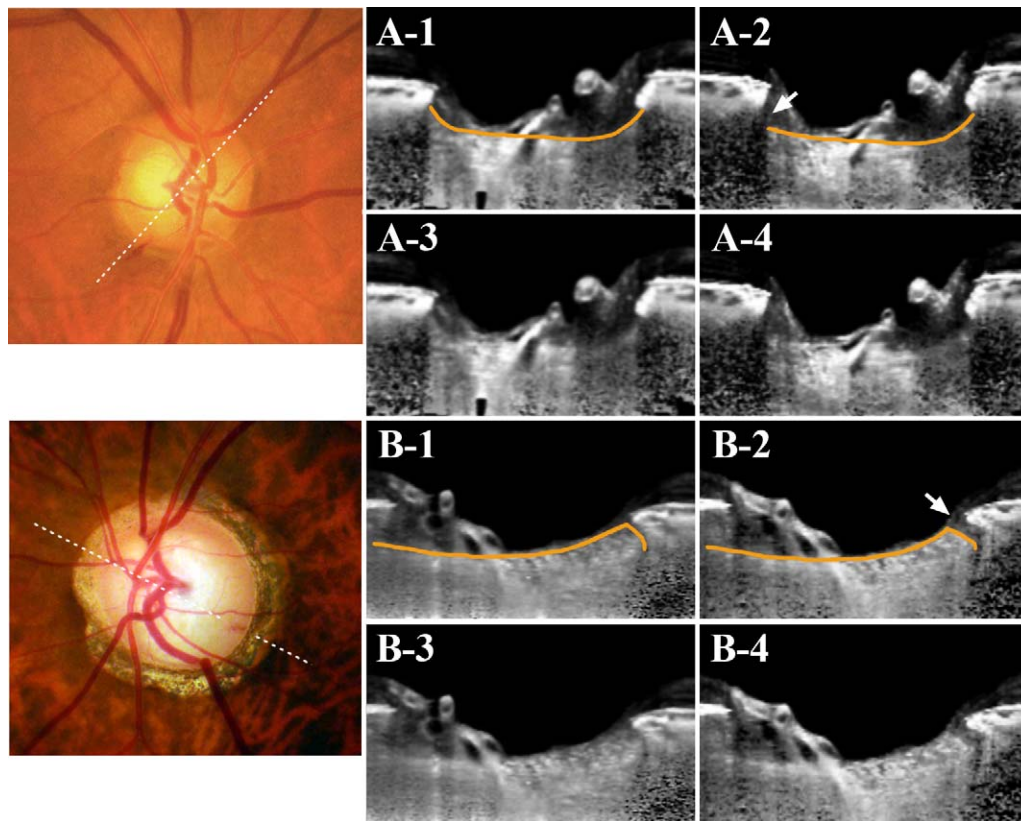
FIGURE 3. Fundus photographs and SD-OCT B-scan images at the meridian (*dotted lines*) of DH. *Left images* (**A-1**, **A-3**, **B-1**, **B-3**) are the baseline B-scans and *right* (**A-2**, **A-4**, **B-2**, **B-4**) are the images obtained after detection of optic disc hemorrhage. *Orange lines* delineate the LC. (**A-3**, **A-4**) Same images as (**A-1**, **A-2**) without labels. (**B-3**, **B-4**) Same images as (**B-1**, **B-2**) without labels. (**A**) Recent structural alteration of the LC with outward deformation of the visible end of anterior LC surface. Note that the visible end of the anterior LC is more posteriorly located in the follow-up image (*arrow*). The change in the curvature of the anterior LC surface also is noticeable (*orange lines*). (**B**) Recent structural alteration of the LC with radial disruption of the temporal LC. Note the enlarged cleft near the LC insertion in the follow up image (or*ange lines* and *arrow*).

sion variability of the measurements was obtained from the images of 20 stable POAG patients who were recruited for our previous study.[44] They were selected among patients who had received treatment and whose IOP had been less than 18 mm Hg with IOP fluctuation < 2 mm Hg during the last 6 months of follow-up. The scan was repeated on a different day within a 1-week period in these patients, and the intraclass correlation coefficient and intersession SD were calculated. A significant change was accepted with an intersession SD of 1.96 times, because it corresponds to the 95% confidence interval for the true value of the measurement.[46]

To define the radial disruption, repeated measure variability was used as a reference instead of test–retest variability, because the cleft was rarely found in patients who can be enrolled as a control for measuring test–retest variability. To calculate the repeated measure variability for the cleft width, an observer measured the width of the cleft twice in separate 20 eyes having visible cleft at the peripheral LC. A significant change was accepted with a repeat measure SD of 1.96 times.

Clinical characteristics and OCT measurements between the groups were compared using independent samples *t*-test, and χ^2 test for continuous variables and categorical variables, respectively. Factors influencing the recent structural alteration of the LC were assessed using logistic regression analysis. Statistical analyses were performed using PASW Statistics 18.0.0 software (SPSS, Chicago, IL, USA). A *P* value of less than 0.05 was considered statistically significant.

RESULTS

We included initially 60 eyes with a DH that was first detected after the baseline SD-OCT optic disc scan. Of these, 15 eyes were excluded because of the poor image quality, which did not allow clear visualization of the temporal LC. For the non-DH group, 49 eyes were included initially. Of these, 13 eyes were excluded for the same reason as in the DH group, leaving a sample of 36 eyes. There were no differences in the baseline clinical characteristics between the two groups, including age, untreated IOP, IOPs at the initial and follow-up scans, IOP fluctuation during the study period, and visual field MD (Table 1).

The intersession reproducibility was excellent for depth of the visible end of anterior LC surface and width of LC cleft measurement (intraclass correlation coefficient = 0.986 and 0.998, respectively). The test–retest variability for the depth of the visible end of anterior LC surface and repeated measure variability for the width of LC cleft were 16.7 and 15.8 μm.

In DH group, the recent LC alteration exceeding the test–retest or repeated measure variability was found in 40 eyes (88.9%). Of these, 11 eyes had recent LC alteration in 1 meridian, 15 eyes in 2 meridians, 7 eyes in 3 meridians, 3 eyes in 4 meridians, and 4 eyes in 5 or more meridians. Thus, the recent LC alteration was found in a total of 95 meridians. Of the 95 meridians, 15 meridians had outward deformation and radial disruption, 48 meridians outward deformation only, and 32 meridians radial disruption only (Table 2). In the non-DH

TABLE 1. Patients' Clinical Demographics

Variables	DH Group, $n = 45$	Non-DH Group, $n = 36$	P Value
Age, y	57.2 ± 13.1 (32 to 81)	53.9 ± 14.4 (21 to 79)	0.288*
Sex, female/male	19/26	14/22	0.762†
Untreated IOP, mm Hg	15.9 ± 3.8 (10 to 25)	15.5 ± 2.5 (10 to 21)	0.553*
IOP at initial scan, mm Hg	12.7 ± 3.0 (7 to 22)	13.0 ± 2.1 (9 to 19)	0.594*
IOP at final scan, mm Hg	12.8 ± 2.7 (9 to 21)	12.7 ± 2.5 (8 to 20)	0.788*
IOP fluctuation, SD‡	1.7 ± 1.0 (0.0 to 4.6)	1.9 ± 0.6 (0.7 to 3.5)	0.257*
RNFL thickness, μm	78.9 ± 13.8 (52 to 110)	75.0 ± 15.3 (42 to 111)	0.230*
Visual field MD, dB	−4.4 ± 4.1 (−16.0 to 0.7)	−5.0 ± 4.7 (−17.1 to 0.6)	0.482*
Visual field PSD, dB	5.5 ± 4.3 (1.5 to 15.4)	5.5 ± 3.8 (1.2 to 14.0)	0.970*
Refractive error, D	−1.4 ± 2.4 (−7.0 to 2.8)	−1.8 ± 2.9 (−8.0 to 1.8)	0.545*
Central corneal thickness, μm	558.6 ± 42.7 (412 to 641)	555.5 ± 42.2 (471 to 632)	0.751*
Axial length, mm	24.5 ± 2.2 (14.6 to 27.9)	24.2 ± 1.6 (21.6 to 27.9)	0.451*
Interval between the initial and follow-up scans, mo	19.7 ± 6.6 (9 to 27)	17.4 ± 7.2 (11 to 36)	0.131
Interval between DH and follow-up scan, mo	8.7 ± 8.3 (0.0 to 22.8)	n/a	n/a

Values are shown in mean ± SD (range). RNFL, retinal nerve fiber layer; PSD, pattern standard deviation; D, diopters.
* The analysis was performed using independent samples t-test.
† The analysis was performed using χ^2 test.
‡ SD of the IOP measurements obtained at 3- or 4-month interval between the initial and final scans.

group, the recent LC alteration was found in four eyes (11.1%). Of these, two, one, and one eyes had the recent LC alteration one, two, and three meridians, respectively. In terms of meridians, the recent LC alteration was found in a total of seven meridians, of which five meridians had outward deformation only and two meridians had radial disruption only.

The central LC depth at the meridians that showed outward deformation did not differ between the initial and follow-up examinations in the DH group (274.91 ± 76.23 vs. 275.41 ± 77.13 μm, $P = 0.721$, paired t-test) and the non-DH group (301.86 ± 76.61 vs. 301.64 ± 75.16 μm, $P = 0.893$, Wilcoxon signed-rank test).

In eyes with recent LC alteration, the amount of maximum outward deformation was larger in the DH group ($n = 33$; 55.82 ± 34.60 μm; range, 17.0–178.7 μm) than in the non-DH group ($n = 3$; 20.15 ± 4.28 μm; range, 16.9–25.0 μm). The amount of maximum radial disruption also was larger in the DH group ($n = 28$; 69.87 ± 46.74 μm; range, 16.2–173.7 μm) than in the non-DH group ($n = 2$, 18.31 ± 1.17 μm; range 17.5–19.1 μm; Fig. 4).

The maximum LC alteration (outward deformation or radial disruption) was observed at the same location as DH in 21 eyes, 0.5 clock-hour apart from the DH in 15 eyes, and 1 clock-hour apart from the DH in 4 eyes (Fig. 5).

Eyes with recent LC alteration had a more frequent prevalence of DH ($P < 0.001$) and a longer axial length ($P = 0.040$) than eyes without LC alteration (Table 3). Univariate logistic regression analysis showed a significant influence of a history of DH (odds ratio = 64.0, $P < 0.001$) and longer axial length (odds ratio = 1.371, $P = 0.049$) on the recent structural LC alteration. In the multivariate analysis, only the history of

TABLE 2. Component of Recent Structural Alteration of the LC in DH and Non-DH Groups

	DH Group, 95 Meridians	Non-DH Group, 7 Meridians
PM (+) and HD (+)	15	0
PM (+) and HD (−)	48	5
PM (−) and HD (+)	32	2

PM, posterior migration of the anterior LC surface; HD, horizontal disruption of the LC.

DH was statistically significant (odds ratio = 59.186, $P < 0.001$, Table 4).

A Representative Case

Figure 6 shows an eye with DH at 10 o'clock, and a noticeable structural alteration of the LC from 9 to 10 o'clock meridians.

DISCUSSION

In the present study, we demonstrated a recent structural alteration of the temporal LC in eyes with DH. The recent LC alteration was located near the DH in all eyes. To our knowledge, this is the first study on the serial observation of the LC configuration in eyes with DH.

Various mechanisms, including ischemic microinfarction at the optic disc,[27–30] blood–retinal barrier dysfunction related with increased circulating cytokines (endothelin-1 or matrix metalloproteinases-9),[31,32] and mechanical rupture of small blood vessels,[22] have been proposed to explain the cause of DH in glaucoma. The mechanical hypothesis[22] proposes that mechanical stress and strain can result in activation of LC astrocytes, which may initiate an immunologic cascade leading to neural and LC tissue degeneration.[13,47–49] Because of the inhomogeneous microarchitecture of the LC, the localized strain on the LC may affect its periphery in particular,[50] and lead to alteration of the peripheral LC. In line with this conception, it has been reported that the mathematical models of the ONH have predicted regions of relatively large mechanical strain in the peripheral LC.[51] In addition, disruption of collagen and elastin at the laminar insertion sites has been demonstrated previously in human and monkey glaucoma.[52] Such alteration may cause rupture of the capillaries inside the peripheral lamina beams. The current finding supports the mechanical hypothesis.

However, there was no difference between the IOPs at the basal ONH scanning and at the follow-up ONH scanning, which was taken after the observation of DH in eyes with recent structural LC alteration. Based on this finding, 2 possibilities may be considered. First, it is possible that the eyes had undetected IOP fluctuation at the time of DH or LC alteration. Second, the LC alteration is not principally resulted from the IOP-related mechanical stress, but is related with a degenerative process of LC induced by other insults. It has
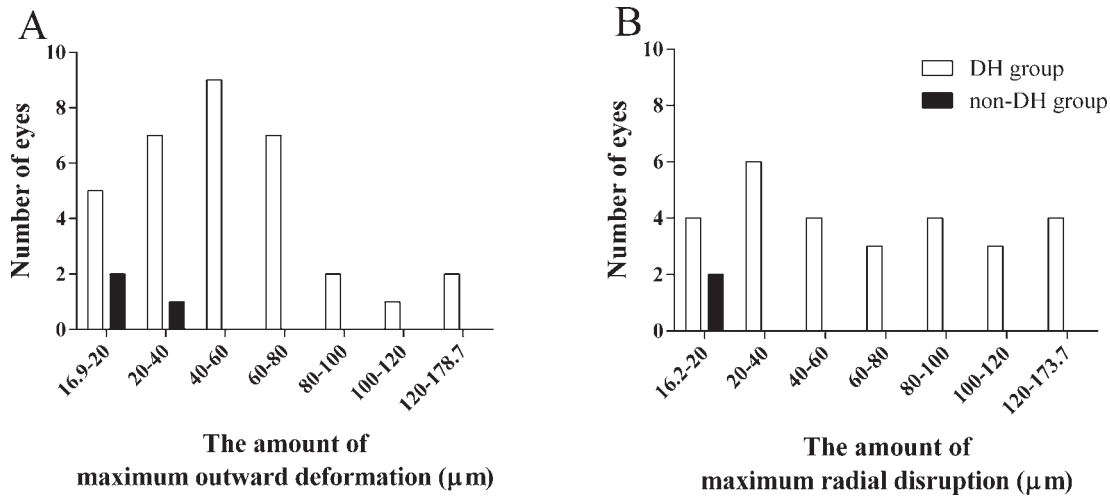
FIGURE 4. Frequency distribution of the maximum amount of an outward deformation of visible end of anterior LC surface (**A**) and a radial disruption (**B**) in the DH group (*white bars*) and non-DH group (*black bars*). Note that only eyes with recent LC alteration were included in this histogram.

been suggested that impaired blood supply to the laminar region may be another factor that can lead to structural changes of the LC, weakening the laminar beams and making them prone to collapse even within a statistically normal range of IOP.[53,54] Alternatively, another scenario involving the ischemic process can be considered. It is possible that DH resulted from microvascular infarction,[27-30] then caused harmful effect in the lamina cribrosa (i.e., degenerative change or increasing the susceptibility to IOP-related stress). In this scenario, alteration of the LC would not be observed at the time of DH, rather gradually developing following DH. In our patients, 13 SD-OCT scans were obtained at the time of first DH after the baseline SD-OCT scan. Of these, 10 eyes showed the recent LC alteration. This finding suggested that DH may be an effect of the LC alteration rather than a cause. However, the possibility should be considered that DH had occurred, but was not detected before in these eyes. A prospective study is

needed to examine the temporal relationship between DH and LC alteration.

The recent LC alteration observed in the current study is in line with histologic studies that showed LC deformation underlies the glaucomatous optic neuropathy.[22-24] In particular, Radius et al.[37] described focal pit-like areas of ectasia in the LC in enucleated eyes with advanced glaucoma. Such defects were located at either the inferior or superior poles of the disc where glaucomatous damage occurs preferentially. Recently, Yang et al.[26] demonstrated the posterior migration of the LC insertion in early experimental glaucomatous monkey eyes. In addition, Girkin et al. (Girkin CA, et al. *IOVS* 2011;52:ARVO E-Abstract 3957) reported disinsertion of the LC in 5 of 14 eyes from 7 donors with open angle glaucoma. The outward deformation in the present study may reflect the posterior migration of the LC insertion at least in some eyes. However, this cannot be confirmed in the present study, because the LC insertion was not always visible. A better technique is needed to confirm this.

Several studies have demonstrated focal LC defect spacially correlated with neuroretinal rim loss,[33,34] visual field defects,[33] and retinal nerve fiber layer defects[35] in glaucomatous eyes. Of note, Park et al.[36] reported that DH was associated with focal LC defects. Our finding suggested that the structural alteration observed in the cross-sectional studies are the result of acquired change rather than congenital deformation.

The change in the XY plane in the B-scan images was designated as radial disruption. It is important to note that such change should have circumferential extent, although this was not demonstrated in the present study. The disruption may involve full thickness LC, leading to the development and/or enlargement of the cleft. When the disruption occurs in partial thickness, a defect may be generated.

In the present study, axial length was associated significantly with LC alteration in the univariate analysis although the association was only marginally significant in the multivariate analysis. This finding is in line with previous observations where the relationship between the myopia and structural defect of the LC was demonstrated.[55,56] Ohno-Matsui et al.[55] and Takayama et al.[56] reported that optic nerve pit or LC defects are more common in eyes with longer axial length. It can be speculated that an increased scleral tension derived from axial elongation might impose mechanical stress on the LC and lead to LC alteration in myopic eyes.
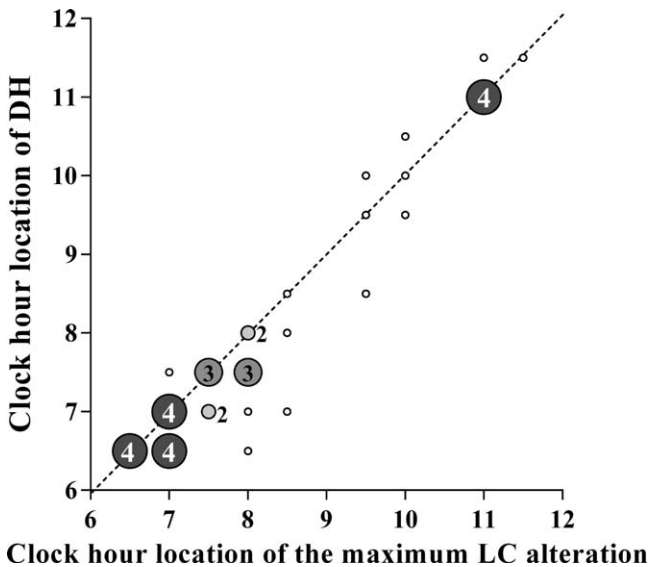

FIGURE 5. The topographic relationship between the location of the maximum LC alteration and the location of DH. The size of each *circle* indicates the number of overlapping data.

TABLE 3. Comparison of Clinical Characteristics Between Eyes With and Without Recent Structural LC Alteration

Variables	Eyes With Recent LC Alteration, $n = 44$	Eyes Without Recent LC Alteration, $n = 37$	P Value
Age, y	57.6 ± 13.2	53.4 ± 14.0	0.167*
Sex, female/male	17/27	16/21	0.674†
History of DH, n (%)	40 (90.9)	5 (13.5)	<0.001†‡
Untreated IOP, mm Hg	15.5 ± 3.7	16.1 ± 2.8	0.438*
IOP at initial scan, mm Hg	12.7 ± 3.0	12.9 ± 2.2	0.626*
IOP at final scan, mm Hg	12.6 ± 2.5	12.9 ± 2.8	0.547*
IOP fluctuation, SD§	1.7 ± 0.9	2.0 ± 0.8	0.215*
RNFL thickness, μm	78.9 ± 13.3	75.1 ± 15.8	0.248*
Visual field MD, dB	−4.3 ± 4.0	−5.1 ± 4.7	0.365*
Visual field PSD, dB	5.2 ± 3.9	5.8 ± 4.2	0.512*
Refractive error, D	−1.7 ± 2.4	−1.4 ± 2.9	0.683*
Central corneal thickness, μm	556.8 ± 43.9	557.5 ± 40.9	0.939*
Axial length, mm	24.8 ± 1.2	23.9 ± 2.3	0.040*‡
Interval between the initial and follow-up scans, mo	19.4 ± 6.5	17.8 ± 7.3	0.292*

Values are shown in mean ± SD (range).
* The analysis was performed using independent samples t-test.
† The analysis was performed using χ^2 test.
‡ Statistically significant values.
§ Standard deviation of the IOP measurements obtained at 3- or 4-month interval between the initial and final scans.

In the non-DH group, patients who had the follow-up optic disc scan within 1 year were included. This was to minimize the possibility of including patients who had undetected DH during the scan interval in the non-DH group. Although each patient's optic disc was examined ophthalmoscopically at each follow-up, it is possible that undetected DH had occurred in between. Such chance will be increased as the interval between the optic disc scans gets longer.

In the present study, eyes with previous DH before the baseline SD-OCT scan were excluded. This was because we were concerned about the possibility that structural alteration of the LC had occurred at the time of previous DH. The vessel wall that ruptured at the time of previous DH might have lost its integrity and became fragile, thereby leading to recurrent episode of DH. In this scenario, further LC alteration does not necessarily occur at the following DH. If this is the case, inclusion of the eyes with previous DH might have induced a bias toward the lower frequency of recent LC alteration in the DH group.

Although Spectralis OCT provides a radial scan protocol, we found that the follow-up images for the radially scanned baseline images often were distorted when obtained using the repeat scan protocol. Thus, we generated the radial scan images from the 3D volume image reconstructed from the raster scan images. From the 3D volume image, one can generate B-scan images at any meridian, freely changing the angle of section, which allowed a comparison at the same meridian between initial and follow-up images. However, the radial scan protocol can provide better image quality. Thus, using the radial scan protocol also may be a good option with careful attention to obtain the images from the same location in each session.

One may argue that the outward deformation of the LC observed in the present study may be an epiphenomenon of backward bowing of the LC. It is possible that the peripheral

TABLE 4. Factors Influencing the Recent Structural LC Alteration

Variables	Univariate			Multivariate		
	Odds Ratio	95% CI	P Value	Odds Ratio	95% CI	P Value
Age, for each y older	1.024	0.990–1.058	0.167			
Female sex	0.826	0.340–2.011	0.674			
History of DH	64.0	15.869–258.119	<0.001*	59.186	13.310–263.183	<0.001*
Untreated IOP, per 1 mm Hg increase	0.947	0.828–1.085	0.434			
IOP at initial scan, per 1 mm Hg increase	0.958	0.810–1.134	0.622			
IOP at final scan, per 1 mm Hg increase	0.949	0.801–1.124	0.542			
IOP fluctuation, per 1 mm Hg increase†	0.717	0.424–1.214	0.216			
RNFL thickness, per 1 μm increase	1.018	0.987–1.051	0.247			
Visual field MD, per 1 dB increase	1.049	0.947–1.162	0.361			
Visual field PSD, per 1 dB increase	0.963	0.863–1.076	0.507			
Refractive error, per 1 diopter increase	0.965	0.815–1.143	0.679			
Central corneal thickness, per 1 μm increase	1.0	0.989–1.010	0.938			
Axial length, per 1 mm increase	1.371	1.001–1.878	0.049*	1.401	0.977–2.009	0.066
Interval between the initial and follow-up scans, per 1 month longer	1.036	0.971–1.105	0.288			

Statistical analysis was performed using logistic regression. CI, confidence interval.
* Statistically significant values.
† Factors with $P < 0.10$ in the univariate analysis were included in the multivariate analysis.
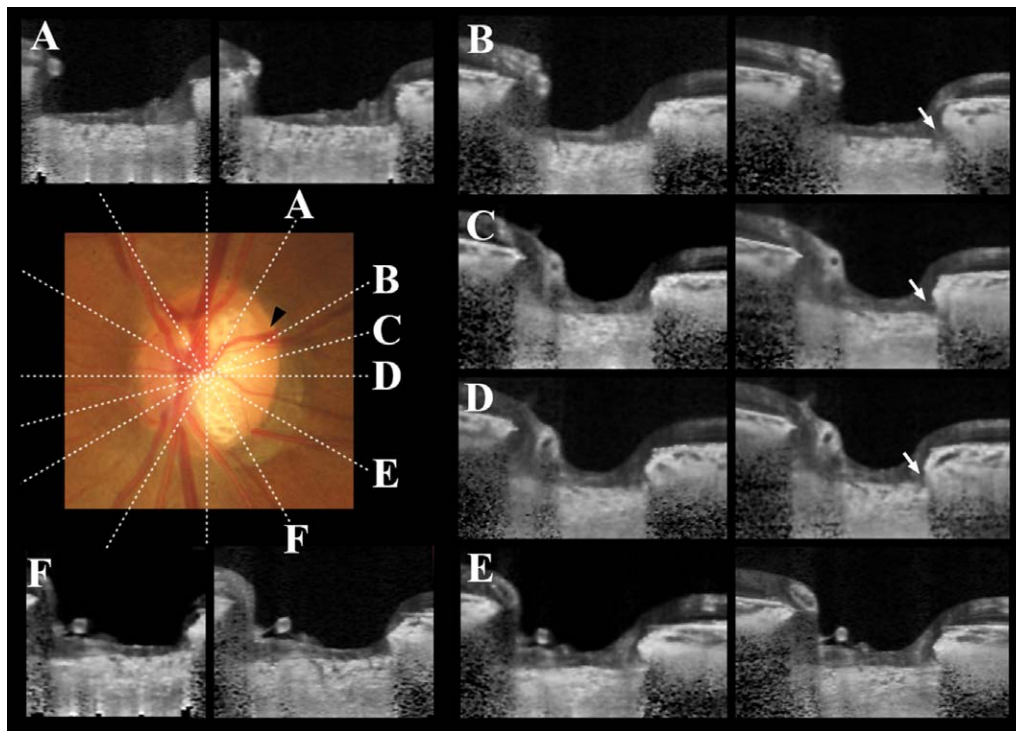
FIGURE 6. Disc photograph and SD-OCT images obtained in the left eye of a 52-year-old woman who had disc DH at 10 o'clock (*arrowhead*). (**A–F**) Radial B-scan images obtained through the direction indicated by *dotted lines* in the color fundus photograph. In each set, the *left images* are pre-DH scan obtained 4 months before detection of DH and the *right images* are post-DH scan obtained 9 months after the DH. (**B–D**) Note the visible change in the configuration of the temporal lamina cribrosa adjacent to the location of DH (*arrows*).

LC moves toward posterior when the LC bows posteriorly. If this was the case, the central LC should have been displaced to larger degree than the amount of outward deformation of the peripheral LC. However, the depth of the central LC was not different between the baseline and follow-up images in eyes showing the outward deformation in the present study. Thus, we considered that the outward deformation of the peripheral LC is a primary event that dynamically occurs at the peripheral LC, independently of the entire LC movement.

The current study has limitations. First, the sample size was small. This is attributable to the low prevalence of DH.[14,17] Despite the small sample size, we observed the distinct difference between the groups in terms of recent structural LC alteration. Second, 25% of eyes with DH, and 27% of eyes without DH were excluded because of the poor visualization of the temporal periphery. Although we applied algorithms including EDI,[38] shadow removal, and contrast enhancement,[40] the techniques still did not provide sufficient image quality to delineate the peripheral LC in all patients. However, even if we assume that all of the 15 excluded eyes from DH group had no LC alteration in the LC, and all of the 13 excluded eyes from the non-DH group had LC alteration, the projected rate of recent LC alteration still is significantly higher in the DH group than in the non-DH group (67.8% vs. 36.0%, $P = 0.001$, χ^2 test). In addition, the degree of observed LC alteration often was markedly larger, in the DH group compared to the non-DH group (Fig. 4), further underlining the difference between the DH and non-DH groups. Further study using technologies that enable better visualization of the LC must be performed. Third, only temporal LC periphery was considered for evaluation in the radial images. This was because of the poor visualization of the nasal half of the LC due to thick neuroretinal rim or overlying large retinal vessels. However, it is known that DH

may occur in the nasal half.[5,14,20,25] Due to the study design, the possibility that recent LC alteration also is involved in the nasal half could not be denied by the current study. A better technique that can visualize the whole LC including the nasal periphery, is needed to examine the alteration in the nasal periphery. Fourth, the non-DH group was matched with the DH group for age, visual field MD, and IOP parameters. This was done to control the potential confounding factors that may be involved in the recent LC alteration. However, this selection of patients may affect the analysis for the factors associated with recent LC alteration. Thus, caution is needed to interpret the results shown in Tables 3 and 4. Further study is needed in the general glaucoma population to elucidate the factors involved in the LC alteration. Lastly, the Fo-BMO axis was not applied to determine the location of the DH. Thus, the clock-hour location of the DH was not defined in an anatomically consistent way among patients. Regardless, this limitation does not affect our study conclusion because the disc photograph and EDI-OCT scan were aligned within each eye.

In conclusion, we demonstrated that a recent structural alteration of the peripheral LC was associated with DH, and that the LC alteration and DH were spatially correlated. While our findings suggested that DH occurs secondary to structural LC alteration, a prospective study is required to elucidate the precise relationship between the DH and the LC alteration.

Acknowledgments

References

1. Budenz DL, Anderson DR, Feuer WJ, et al. Detection and prognostic significance of optic disc hemorrhages during the Ocular Hypertension Treatment Study. *Ophthalmology*. 2006; 113:2137–2143.

2. Miglior S, Torri V, Zeyen T, et al. Intercurrent factors associated with the development of open-angle glaucoma in the European glaucoma prevention study. *Am J Ophthalmol*. 2007;144:266–275.

3. Drance S, Anderson DR, Schulzer M. Collaborative Normal-Tension Glaucoma Study G. Risk factors for progression of visual field abnormalities in normal-tension glaucoma. *Am J Ophthalmol*. 2001;131:699–708.

4. Leske MC, Heijl A, Hussein M, et al. Factors for glaucoma progression and the effect of treatment: the early manifest glaucoma trial. *Arch Ophthalmol*. 2003;121:48–56.

5. Siegner SW, Netland PA. Optic disc hemorrhages and progression of glaucoma. *Ophthalmology*. 1996;103:1014–1024.

6. Rasker MT, van den Enden A, Bakker D, Hoyng PF. Deterioration of visual fields in patients with glaucoma with and without optic disc hemorrhages. *Arch Ophthalmol*. 1997; 115:1257–1262.

7. Ishida K, Yamamoto T, Sugiyama K, Kitazawa Y. Disk hemorrhage is a significantly negative prognostic factor in normal-tension glaucoma. *Am J Ophthalmol*. 2000;129:707–714.

8. Kim SH, Park KH. The relationship between recurrent optic disc hemorrhage and glaucoma progression. *Ophthalmology*. 2006;113:598–602.

9. Bengtsson B, Leske MC, Yang Z, Heijl A. Group E. Disc hemorrhages and treatment in the early manifest glaucoma trial. *Ophthalmology*. 2008;115:2044–2048.

10. Sugiyama K, Tomita G, Kitazawa Y, Onda E, Shinohara H, Park KH. The associations of optic disc hemorrhage with retinal nerve fiber layer defect and peripapillary atrophy in normal-tension glaucoma. *Ophthalmology*. 1997;104:1926–1933.

11. Sugiyama K, Uchida H, Tomita G, Sato Y, Iwase A, Kitazawa Y. Localized wedge-shaped defects of retinal nerve fiber layer and disc hemorrhage in glaucoma. *Ophthalmology*. 1999;106: 1762–1767.

12. Gunvant P, Zheng Y, Essock EA, et al. Predicting subsequent visual field loss in glaucomatous subjects with disc hemorrhage using retinal nerve fiber layer polarimetry. *J Glaucoma*. 2005;14:20–25.

13. Hernandez MR. The optic nerve head in glaucoma: role of astrocytes in tissue remodeling. *Prog Retin Eye Res*. 2000;19: 297–321.

14. Diehl DL, Quigley HA, Miller NR, Sommer A, Burney EN. Prevalence and significance of optic disc hemorrhage in a longitudinal study of glaucoma. *Arch Ophthalmol*. 1990;108: 545–550.

15. Klein BE, Klein R, Sponsel WE, et al. Prevalence of glaucoma. The Beaver Dam Eye Study. *Ophthalmology*. 1992;99:1499–1504.

16. Hendrickx KH, van den Enden A, Rasker MT, Hoyng PF. Cumulative incidence of patients with disc hemorrhages in glaucoma and the effect of therapy. *Ophthalmology*. 1994; 101:1165–1172.

17. Jonas JB, Xu L. Optic disk hemorrhages in glaucoma. *Am J Ophthalmol*. 1994;118:1–8.

18. Healey PR, Mitchell P, Smith W, Wang JJ. Optic disc hemorrhages in a population with and without signs of glaucoma. *Ophthalmology*. 1998;105:216–223.

19. Suh MH, Park KH. Period prevalence and incidence of optic disc haemorrhage in normal tension glaucoma and primary open-angle glaucoma. *Clin Exp Ophthalmol*. 2011;39:513–519.

20. Airaksinen PJ, Mustonen E, Alanko HI. Optic disc hemorrhages. Analysis of stereophotographs and clinical data of 112 patients. *Arch Ophthalmol*. 1981;99:1795–1801.

21. Airaksinen PJ, Mustonen E, Alanko HI. Optic disc haemorrhages precede retinal nerve fibre layer defects in ocular hypertension. *Acta Ophthalmol*. 1981;59:627–641.

22. Quigley HA, Addicks EM, Green WR, Maumenee AE. Optic nerve damage in human glaucoma. II. The site of injury and susceptibility to damage. *Arch Ophthalmol*. 1981;99:635–649.

23. Emery JM, Landis D, Paton D, Boniuk M, Craig JM. The lamina cribrosa in normal and glaucomatous human eyes. *Trans Am Acad Ophthalmol Otolaryngol*. 1974;78:OP290–OP297.

24. Radius RL, Gonzales M. Anatomy of the lamina cribrosa in human eyes. *Arch Ophthalmol*. 1981;99:2159–2162.

25. Nitta K, Sugiyama K, Higashide T, Ohkubo S, Tanahashi T, Kitazawa Y. Does the enlargement of retinal nerve fiber layer defects relate to disc hemorrhage or progressive visual field loss in normal-tension glaucoma? *J Glaucoma*. 2011;20:189–195.

26. Yang H, Williams G, Downs JC, et al. Posterior (outward) migration of the lamina cribrosa and early cupping in monkey experimental glaucoma. *Invest Ophthalmol Vis Sci*. 2011;52: 7109–7121.

27. Drance SM, Begg IS. Sector haemorrhage—a probable acute ischaemic disc change in chronic simple glaucoma. *Can J Ophthalmol*. 1970;5:137–141.

28. Begg IS, Drance SM, Sweeney VP. Haemorrhage on the disc—a sign of acute ischaemic optic neuropathy in chronic simple glaucoma. *Can J Ophthalmol*. 1970;5:321–330.

29. Begg IS, Drance SM, Sweeney VP. Ischaemic optic neuropathy in chronic simple glaucoma. *Br J Ophthalmol*. 1971;55:73–90.

30. Lichter PR, Henderson JW. Optic nerve infarction. *Am J Ophthalmol*. 1978;85:302–310.

31. Grieshaber MC, Terhorst T, Flammer J. The pathogenesis of optic disc splinter haemorrhages: a new hypothesis. *Acta Ophthalmol Scand*. 2006;84:62–68.

32. Golubnitschaja O, Yeghiazaryan K, Liu R, et al. Increased expression of matrix metalloproteinases in mononuclear blood cells of normal-tension glaucoma patients. *J Glaucoma*. 2004;13:66–72.

33. Kiumehr S, Park SC, Syril D, et al. In vivo evaluation of focal lamina cribrosa defects in glaucoma. *Arch Ophthalmol*. 2012; 130:552–559.

34. You JY, Park SC, Su D, Teng CC, Liebmann JM, Ritch R. Focal lamina cribrosa defects associated with glaucomatous rim thinning and acquired pits. *JAMA Ophthalmol*. 2013;131:314–320.

35. Tatham AJ, Miki A, Weinreb RN, Zangwill LM, Medeiros FA. Defects of the lamina cribrosa in eyes with localized retinal nerve fiber layer loss. *Ophthalmology*. 2014;121:110–118.

36. Park SC, Hsu AT, Su D, et al. Factors associated with focal lamina cribrosa defects in glaucoma. *Invest Ophthalmol Vis Sci*. 2013;54:8401–8407.

37. Radius RL, Maumenee AE, Green WR. Pit-like changes of the optic nerve head in open-angle glaucoma. *Br J Ophthalmol*. 1978;62:389–393.

38. Spaide RF, Koizumi H, Pozzoni MC. Enhanced depth imaging spectral-domain optical coherence tomography. *Am J Ophthalmol*. 2008;146:496–500.

39. Lee EJ, Kim TW, Weinreb RN, Park KH, Kim SH, Kim DM. Visualization of the lamina cribrosa using enhanced depth imaging spectral-domain optical coherence tomography. *Am J Ophthalmol*. 2011;152:87–95.

40. Girard MJ, Strouthidis NG, Ethier CR, Mari JM. Shadow removal and contrast enhancement in optical coherence tomography images of the human optic nerve head. *Invest Ophthalmol Vis Sci*. 2011;52:7738–7748.

41. Foin N, Mari JM, Davies JE, Di Mario C, Girard MJ. Imaging of coronary artery plaques using contrast-enhanced optical coherence tomography. *Eur Heart J Cardiovasc Imaging*. 2013;14:85.

42. Lee EJ, Kim TW, Weinreb RN, et al. Three-dimensional evaluation of the lamina cribrosa using spectral-domain optical coherence tomography in glaucoma. *Invest Ophthalmol Vis Sci*. 2012;53:198–204.

43. Lee EJ, Kim TW, Weinreb RN. Reversal of lamina cribrosa displacement and thickness after trabeculectomy in glaucoma. *Ophthalmology*. 2012;119:1359–1366.

44. Lee EJ, Kim TW, Weinreb RN, Kim H. Reversal of lamina cribrosa displacement after intraocular pressure reduction in open-angle glaucoma. *Ophthalmology*. 2013;120:553–559.

45. Chauhan BC, Burgoyne CF. From clinical examination of the optic disc to clinical assessment of the optic nerve head: a paradigm change. *Am J Ophthalmol*. 2013;156:218–227.

46. Jampel HD, Vitale S, Ding Y, et al. Test-retest variability in structural and functional parameters of glaucoma damage in the glaucoma imaging longitudinal study. *J Glaucoma*. 2006; 15:152–157.

47. Burgoyne CF, Downs JC, Bellezza AJ, Suh JK, Hart RT. The optic nerve head as a biomechanical structure: a new paradigm for understanding the role of IOP-related stress and strain in the pathophysiology of glaucomatous optic nerve head damage. *Prog Retin Eye Res*. 2005;24:39–73.

48. Quill B, Docherty NG, Clark AF, O'Brien CJ. The effect of graded cyclic stretching on extracellular matrix-related gene expression profiles in cultured primary human lamina cribrosa cells. *Invest Ophthalmol Vis Sci*. 2011;52:1908–1915.

49. Yang J, Yang P, Tezel G, Patil RV, Hernandez MR, Wax MB. Induction of HLA-DR expression in human lamina cribrosa astrocytes by cytokines and simulated ischemia. *Invest Ophthalmol Vis Sci*. 2001;42:365–371.

50. Park SC, Kiumehr S, Teng CC, Tello C, Liebmann JM, Ritch R. Horizontal central ridge of the lamina cribrosa and regional differences in laminar insertion in healthy subjects. *Invest Ophthalmol Vis Sci*. 2012;53:1610–1616.

51. Crawford Downs J, Roberts MD, Sigal IA. Glaucomatous cupping of the lamina cribrosa: a review of the evidence for active progressive remodeling as a mechanism. *Exp Eye Res*. 2011;93:133–140.

52. Quigley HA, Dorman-Pease ME, Brown AE. Quantitative study of collagen and elastin of the optic nerve head and sclera in human and experimental monkey glaucoma. *Curr Eye Res*. 1991;10:877–888.

53. Arend O, Plange N, Sponsel WE, Remky A. Pathogenetic aspects of the glaucomatous optic neuropathy: fluorescein angiographic findings in patients with primary open angle glaucoma. *Brain Res Bull*. 2004;62:517–524.

54. Downs JC, Roberts MD, Burgoyne CF. Mechanical environment of the optic nerve head in glaucoma. *Optom Vis Sci*. 2008;85: 425–435.

55. Ohno-Matsui K, Akiba M, Moriyama M, et al. Acquired optic nerve and peripapillary pits in pathologic myopia. *Ophthalmology*. 2012;119:1685–1692.

56. Takayama K, Hangai M, Kimura Y, et al. Three-dimensional imaging of lamina cribrosa defects in glaucoma using swept-source optical coherence tomography. *Invest Ophthalmol Vis Sci*. 2013;54:4798–4807.